

## Supporting Information

### Ultrasensitive and Stretchable Resistive Strain Sensors Designed for Wearable Electronics

Xinqin Liao,<sup>a</sup> Zheng Zhang,<sup>a</sup> Zhuo Kang,<sup>a</sup> Fangfang Gao,<sup>a</sup> Qingliang Liao\*<sup>a</sup> and Yue Zhang\*<sup>ab</sup>

<sup>a</sup> State Key Laboratory for Advanced Metals and Materials, School of Materials Science and Engineering, University of Science and Technology Beijing, Beijing 100083, People's Republic of China

E-mail: [yuezhang@ustb.edu.cn](mailto:yuezhang@ustb.edu.cn); [liao@ustb.edu.cn](mailto:liao@ustb.edu.cn).

<sup>b</sup> The Beijing Municipal Key Laboratory of New Energy Materials and Technologies, University of Science and Technology Beijing, Beijing 100083, People's Republic of China

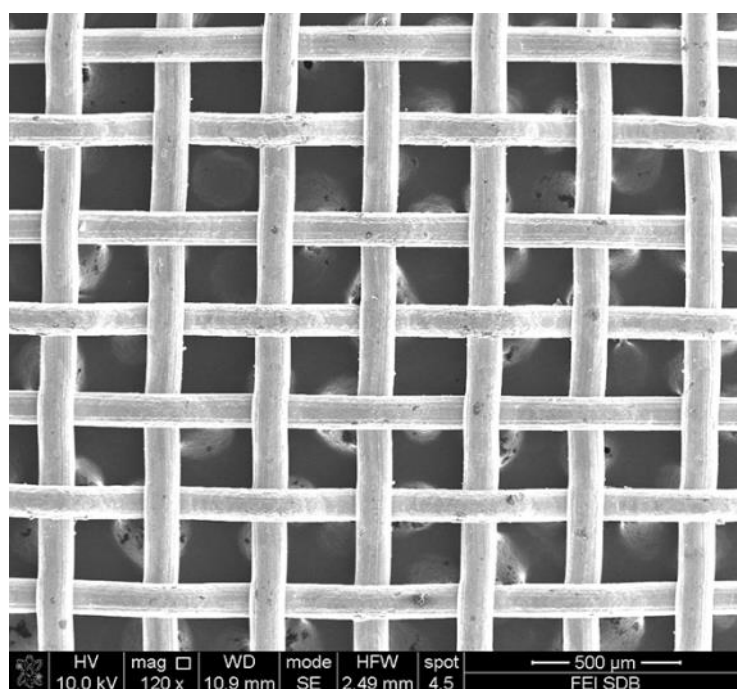


**Fig. S1.** SEM image of a piece of steel net. It can be observed that the steel lines are parallel to each other, and regular.

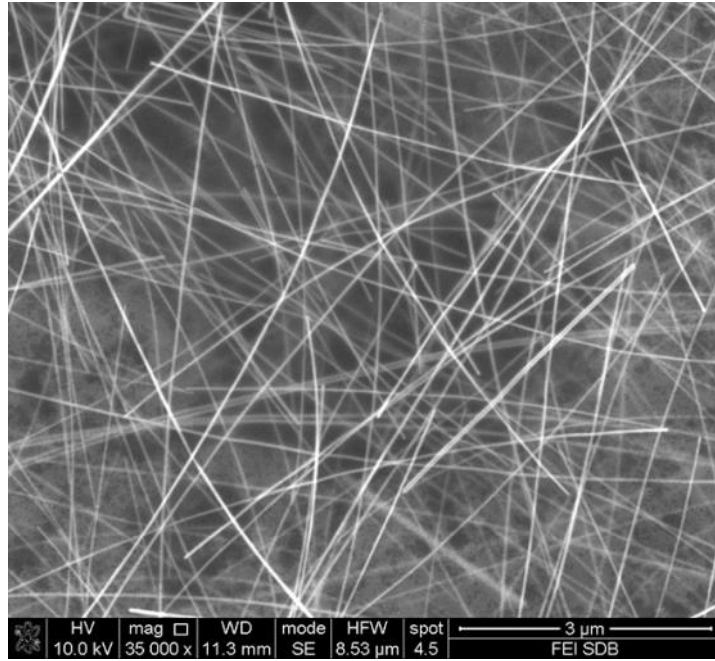


**Fig. S2.** SEM image of Ag NWs. It can be observed that the Ag NWs possesses large length-diameter ratio. It is helpful to the formation of a good percolating conductive path.

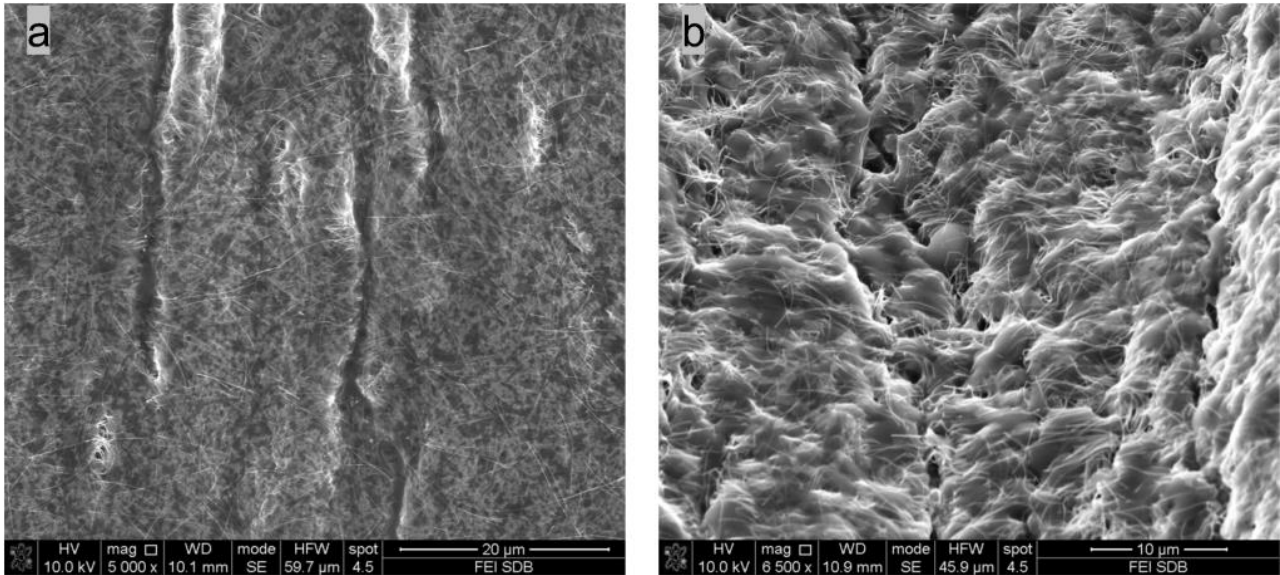


**Fig. S3.** SEM images of (a) square plat and (b) concave line of Ag NWs@P-PDMS. It can be observed that plenty of microcracks widely exists in the surface of the P-PDMS no matter outside the square plats and inside parallel concave lines.

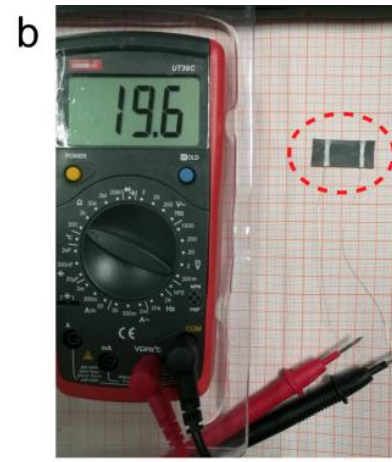
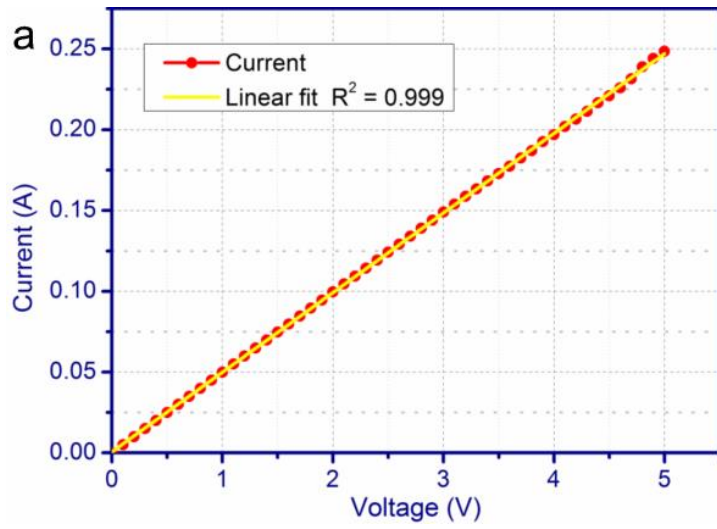


**Fig. S4. (a)** Typical current-voltage characteristic of the strain sensor. **(b)** The original electrical resistance of the strain sensor. From the two measurements, it can be known that the original resistance of the strain sensor is relatively low.

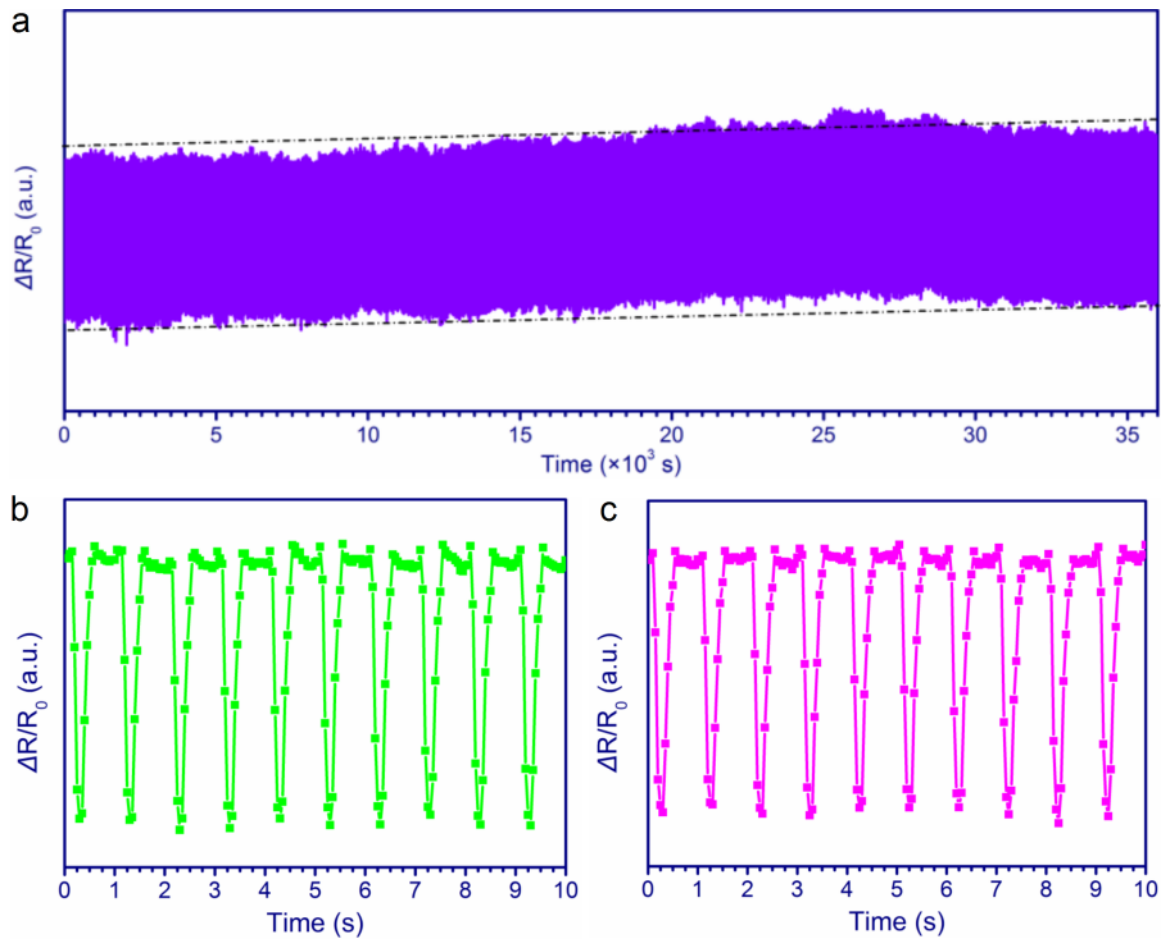


**Fig. S5.** (a) Variations in resistance of the strain sensor for > 35 000 strain loading-unloading cycles from 5% to 25% at the stretching frequency of 1 Hz. (b) The continuous strain responses at the time of the first ten seconds (c) The relative resistance changes of the strain sensor to the applied strain after 35 000 strain loading-unloading cycles.

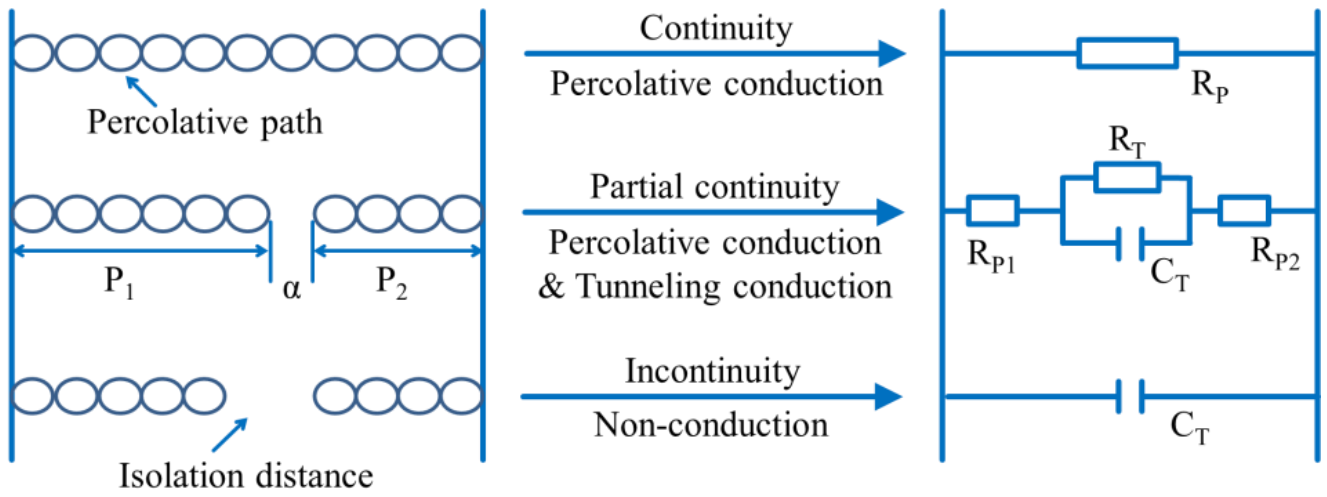


**Fig. S6.** The models and analog circuits of three internal structures of Ag NWs@P-PDMS.

We classified internal structures of Ag NWs@P-PDMS, surface conductive composite polymers, into three types depending on isolation distance of each percolative path: (I) complete continuity with no isolation distance, (II) partial continuity with a certain isolation distance, (III) complete disconnection between each percolative path. Correspondingly, the conductive strategies are based on percolative conduction, percolative conduction with tunneling conduction, and non-conduction. In this way, the total resistance  $R_{total}$  can be calculated by using Kirchhoff's circuit law and Ohm's law, which are  $R_{total} = \sum R_p$  (S1),  $R_{total} = \sum(R_p + R_T)$  (S2) and  $R_{total} \rightarrow \infty$  (S3), respectively, where  $R_p$  is the resistance of percolative path,  $R_T$  is the tunneling resistance.

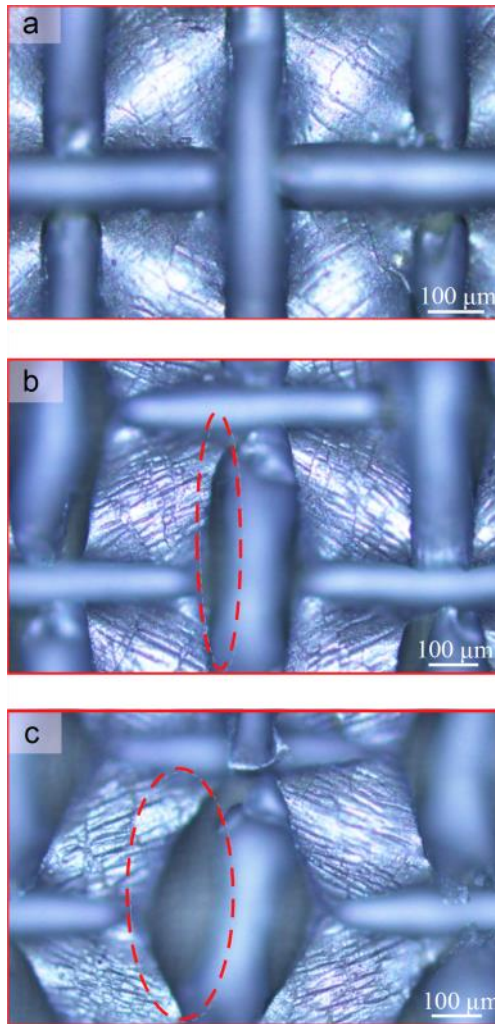


**Fig. S7.** The SEM images of the strain sensor (a) without or with (b) small and (c) large applied strain. The SEM images are the original ones of Figure 5.

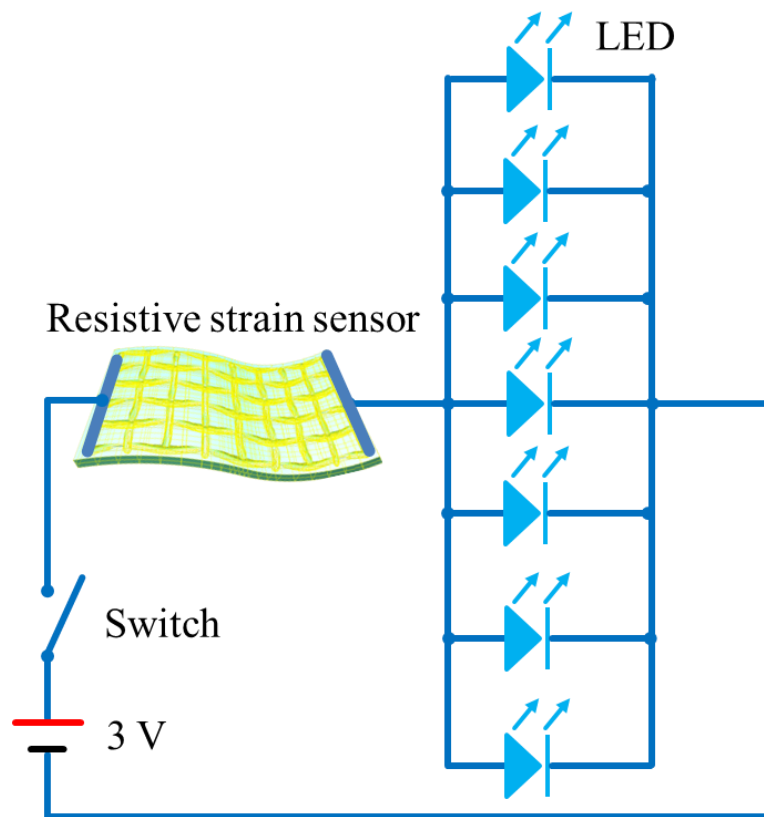


**Fig. S8.** The series-parallel circuit of the control system of a LED indicator. Through a simple arrangement and layout, the LEDs can be formed to be a LED indicator just like Figure 6.



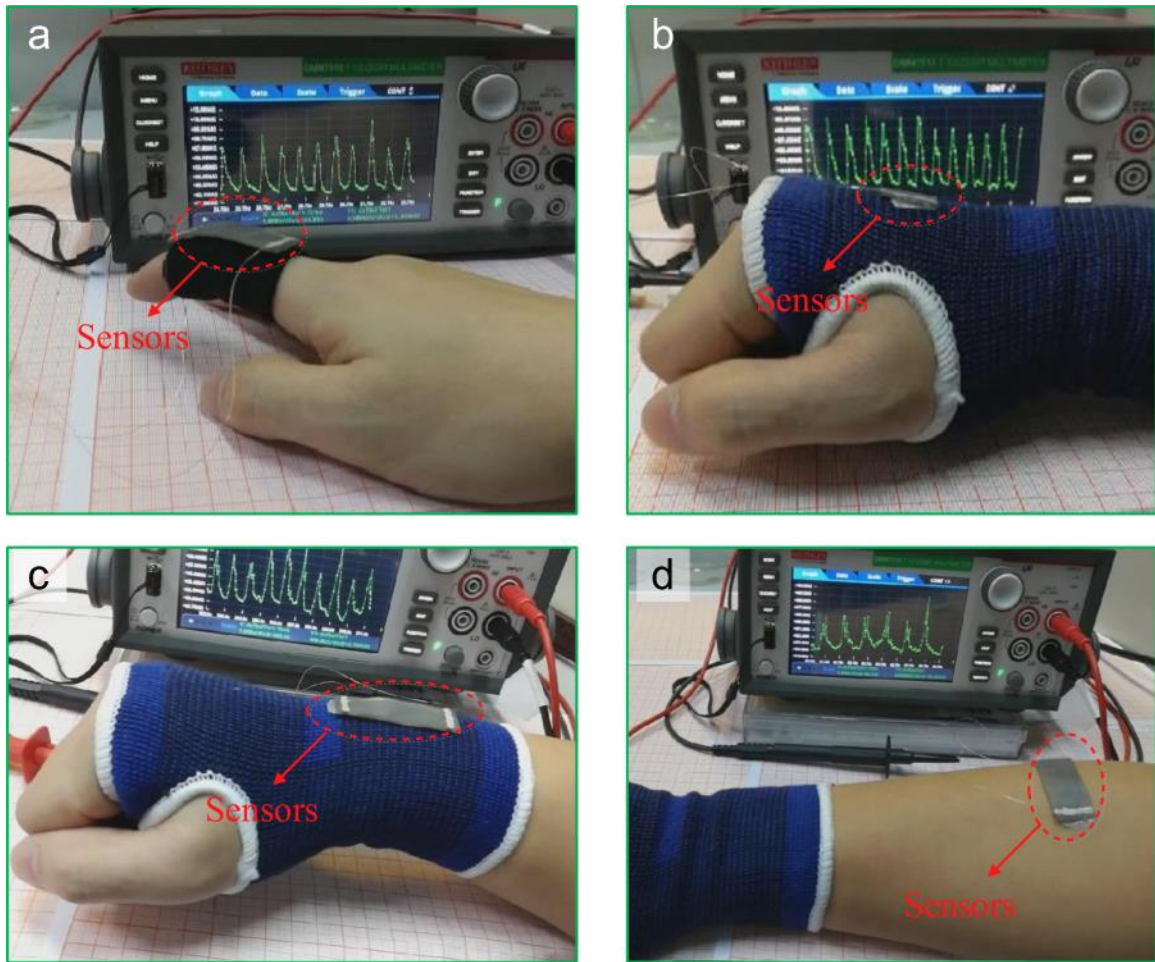


**Fig. S9.** Photographs of the movie clip for the application of (a) smart fingerstall, (b) smart hand protector, (c) functional wrister and (d) electronic skin.